Optical Heterodyne Generation of High-Dimensional and Broadband White Chaos

Anbang Wang, *Member, IEEE*, Bingjie Wang, Lei Li, Yuncai Wang, and K. Alan Shore, *Senior Member, IEEE*

***Abstract*—White chaos with a colorless spectral bandwidth of 14 GHz contained within a range of 3 dB is experimentally generated by optical heterodyning of two external-cavity laser diodes. Experimental and numerical results show that the signatures of laser relaxation oscillation and external-cavity resonance (i.e., time delay signature), which are intrinsic to the laser dynamics are totally eliminated in the heterodyne-generated chaos. Correlation dimensional analysis shows that the generated chaos has a high dimensionality, being greater than 10. In addition, the effects on the heterodyne spectral bandwidth of variations in the optical feedback strength and frequency detuning of the lasers are studied experimentally and theoretically. Opportunities are identified for the deployment of white chaos.**

***Index Terms*—Chaos, heterodyning, optical feedback, semiconductor lasers, white noise.**

I. Introduction

APPLICATION of laser chaos in fast physical random bit generation has attracted intensive attention since Uchida *et al*. generated 1.7 Gb/s random bits using chaotic external-cavity semiconductor lasers (ECLs) with single-bit extraction [1]. The speed of random number generation can be further multiplied by using multi-bit extraction with assistance of derivative or XOR operation [2]–[4]. It is worth noting that the single-bit generation rate is the fundamental rate physically determined by the entropy rate of chaos which is related to bandwidth and flatness of the spectrum [5], [6]. Unfortunately, the ECL has two intrinsic oscillations that limit the bandwidth and flatness of spectrum of chaotic output. One is the laser relaxation oscillation that dominates the laser chaos and then limits the effective bandwidth only to a few gigahertz [7]. The other is the external-cavity resonance that gives rise to a periodic modulation pattern in the power spectrum and causes a high correlation value at the time delay (i.e., time delay signature) [8]–[10]. Much effort has been devoted to enhancing bandwidth [6], [11], [12], because bandwidth enhancement can shorten the correlation time of chaotic waveform and physically increase the sampling rate, and then can greatly improve the maximum speed with multi-bit generation. In addition, to eliminate the time delay signature, other ways of generating chaos without delayed feedback have been suggested, such as optical injection [13] or polarization mode competition [4], although the generated spectrum is narrow and features the relaxation oscillation. It is therefore interesting to establish whether an alternative method can generate a broadband chaos having a flat and wide spectrum without signatures of intrinsic frequencies such as relaxation oscillations and external-cavity resonance.

It has been reported that the power spectrum of chaotic ECL can be expanded by means of additional optical injection [7], [14]–[19]. The signature of feedback delay can be depressed by other approaches, such as proper adjustment of the feedback parameters [20] and complex feedback schemes including dual-cavity feedback [21], polarization-rotated feedback [22], [23], and grating feedback [24]. Unfortunately, these methods cannot simultaneously eliminate the domination of relaxation oscillation and the signature of external-cavity resonance to achieve a chaos with a uniform spectrum.

Note that, chaos with such a uniform spectrum like a white noise is referred to as white chaos [25]. The generation of white chaos has been reported in some mathematical maps such as the piecewise-linear Markov map [25] and the Logistic map [26]. However, the spectral width achieved via electronic circuit realizations of such mathematical maps is extremely limited being of order a few kilohertz [26]. This is entirely inadequate for practical applications. In this paper we experimentally and numerically demonstrate a scheme for generating white chaos with a bandwidth greater than 10 GHz. The approach taken is to effect an optical heterodyning of two ECLs.

Previously we showed that phase-to-intensity conversion for a chaotic ECL by delayed self-interference can eliminate the relaxation-oscillation feature, but the generated self-interference signal has a downward-sloping spectrum with a small bandwidth and still has the time delay signature [27]. The optical heterodyne method we present here is an improved scheme for generating white chaos. This method not only can eliminate the feature of the laser relaxation oscillation but also can realize a flat spectrum with large bandwidth by adjusting the frequency detuning between the two ECLs. Simultaneously, the method can conceal the signature of external-cavity resonance or feedback delay by ensuring that the two external-cavity lengths are incommensurate.

Manuscript received January 20, 2015; revised April 3, 2015; accepted April 24, 2015. This work was supported in part by the National Natural Science Foundation of China under Grants 60908014, 61205142, 61227016, and 61475111, in part by the International Science and Technology Cooperation Program of China under Grant 2014DFA50870, in part by the Key Program for Shanxi Innovative Research Team for Science and Technology under Grant 2013091021, in part by the Program for the Innovative Talents of Higher Learning Institutions of Shanxi, and in part by the Program for Excellent Talents in Taiyuan University of Technology under Grant 2014YQ001.

A. Wang, B. Wang, L. Li, and Y. Wang are with the Key Laboratory of Advanced Transducers and Intelligent Control System, Ministry of Education and Shanxi Province, and College of Physics and Optoelectronics, Taiyuan University of Technology, Taiyuan 030024, China (e-mail: wanganbang@tyut.edu.cn; wbj1131@163.com; 18234132836@139.com; wangyc@tyut.edu.cn).

K. A. Shore is with the School of Electronic Engineering, Bangor University, Bangor LL57 1UT, U.K. (e-mail: k.a.shore@bangor.ac.uk).

Color versions of one or more of the figures in this paper are available online at http://ieeexplore.ieee.org.

Digital Object Identifier 10.1109/JSTQE.2015.2427253

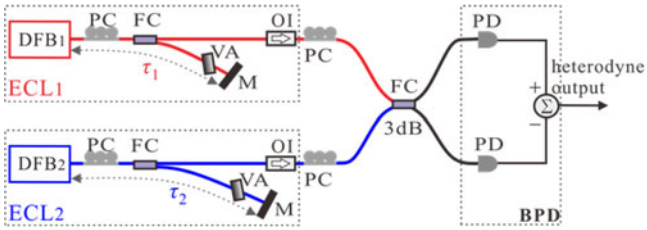

Fig. 1. Experimental setup of white chaos generation using the optical heterodyning of two external-cavity feedback lasers (ECLs). Each ECL consists of a DFB semiconductor laser with optical feedback from a fiber mirror (M). τ_1, τ_2 are the round-trip time in feedback cavities. PC: polarization controller; FC: fiber coupler; VA: variable attenuation; OI: optical isolator; PD: photodetector; BPD: balanced photodetector.

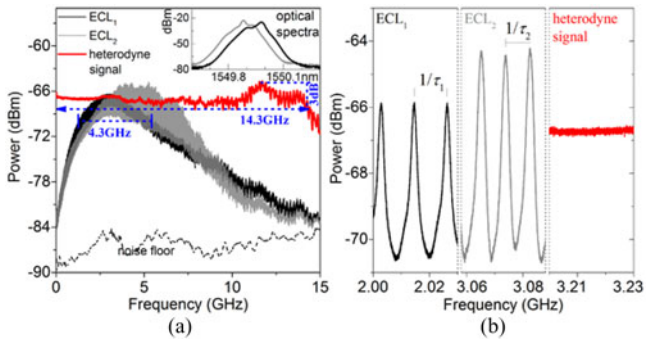

Fig. 2. Experimental RF spectra of an optical heterodyne signal and intensity chaos of ECLs in different frequency scales, (a) 15 GHz and (b) 30 MHz. The inset plots the optical spectra of the two ECLs. Black: ECL_1; light gray: ECL_2; gray (red online): the heterodyne signal. Resolution bandwidth: 1 MHz; video bandwidth: 3 kHz; sweep time: 1 s. Experimental conditions are listed in the text.

This paper is organized as follows: the experimental arrangement utilized is described in the next section and experimental results obtained are then presented. A theoretical model of the experimental arrangement is outlined and a comparison is made between predictions of the model and the measurements. Analyses of correlation dimension (CD) and memory time for the generated white chaos is then offered in the section of discussion and the paper ends with a brief conclusion which indicates scope for practical utilization of the scheme presented here.

II. Experimental Arrangement

The experimental arrangement is presented in Fig. 1. As shown in the dashed boxes, each ECL consists of a distributed feedback (DFB) semiconductor laser subject to optical feedback from a fiber mirror. The laser facet and the fiber mirror comprise a feedback cavity. In the feedback cavity, a polarization controller is used to match the polarization of the feedback light to that of the laser, and an optical variable attenuator is utilized to adjust the feedback strength to change the dynamic state of the laser. It is noted that the feedback strength is defined as the power ratio of the feedback light to the laser output. The feedback delay time (i.e., round-trip time in the feedback cavities) of ECL_1 and ECL_2 are denoted as τ_1 and τ_2, respectively. The two delays are taken to be incommensurate, that is, $q\tau_1 \neq p\tau_2$, for any positive integers q and p. The outputs of the two ECLs are coupled through a 3-dB fiber coupler, and their heterodyne signal is subsequently extracted by a balanced detector.

In the experiments, the lasers DFB_1 and DFB_2 (WTD LDM5 S752) have threshold values of 10.3 mA and 11.0 mA, respectively, and both are biased at 14.8 mA by laser drivers (ILX Lightwave LDX-3412). The lasers' wavelengths are stabilized and tuned by temperature controllers (ILX Lightwave LDT-5412). The two feedback delays are $\tau_1 = 85.3$ ns and $\tau_2 = 110.7$ ns, respectively. A fast balanced photodetector with a bandwidth of 40 GHz (Discovery DSC R410), in which two identical photodetectors and an electronic circuit are integrated, is used to extract the heterodyne signal. An optical tunable delay line (General Photonics, MDL-002) that has a resolution of less than 0.3μm is used to minimize the optical path difference between the two fiber paths before the balanced detector. The heterodyne signal is measured by a radio-frequency (RF) spectrum analyzer (Agilent N9020 A) and a 6-GHz bandwidth real-time oscilloscope (LeCroy SDA 806 Zi-A). The optical spectra of the ECLs are measured by an optical spectrum analyzer with a resolution of 0.02 nm (YOKOGAWA AQ6370 C).

III. Experimental Results

A. White Chaos Generation

In this section results demonstrating the experimental generation of white chaos are presented and the dynamical properties of the chaos thus generated are characterized. These representative results are obtained with the following parameters: feedback strengths $\kappa_1 = -15.9$ dB and $\kappa_2 = -19.5$ dB and the lasers' center wavelengths $\lambda_1 = 1549.980$ nm and $\lambda_2 = 1549.882$ nm.

Fig. 2(a) shows the RF spectrum of the heterodyne signal as the gray (red online) line as well as the spectra of the intensity chaos of ECL_1 and ECL_2 as the black and light gray lines, respectively, in a scale of 15 GHz. Fig. 2(b) shows the corresponding fine spectra in a small scale of 30 MHz. According to the optical spectra of the ECLs plotted in the inset of Fig. 2(a), the laser linewidth at –10 dB of ECL_1 and ECL_2 is about 20 and 16 GHz, respectively, which are greater than the linewidth of the solitary DFB lasers. The reason is that the optical feedback induces many external-cavity modes (ECMs) into laser field and thus broadens the optical spectrum [28]. Note that the ECMs cannot be seen in the measured optical spectra due to the limitation of resolution of the used optical spectrum analyzer.

From the black or gray lines in Fig. 2(a), it is found that the spectrum of laser intensity chaos covers a wide frequency range of 15 GHz. However, the spectrum has an obvious peak approximately at the laser relaxation oscillation frequency, the peak being approximately 18 dB higher than the lowest spectral component. That is, the whole spectrum is dominated or is colored by the relaxation oscillation frequency. In addition, as shown in the left two panels in Fig. 2(b), the fine spectra exhibit a pattern of periodic modulation with a depth of greater than 5 dB. The modulation period equals the reciprocal of the delay time. This means that the spectrum of laser intensity chaos is also locally colored by the resonance of external feedback cavity.

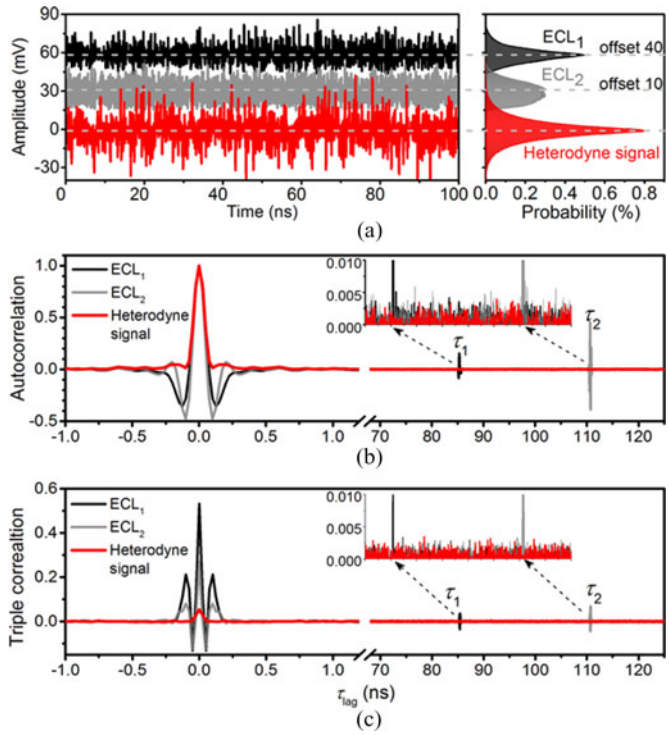

Fig. 3. Temporal statistical properties of the experimental heterodyne signal as well as the intensity chaos of ECLs shown in Fig. 2: (a) time series (left) and amplitude probability distributions (right), (b) ACFs, and (c) TCFs (Black: ECL_1; light gray: ECL_2; gray (red): the heterodyne signal). Correlation length is 2×10^6 points.

By contrast, shown in gray (red) line in Fig. 2(a) the RF spectrum of the optical heterodyne signal is very flat over a wide frequency band and is free of dominant peaks. Specifically, the spectrum is contained with a power range of 3 dB for frequencies up to 14.3 GHz. Furthermore, the fine spectrum in the right panel in Fig. 2(b) is also flat without periodic modulation pattern. Therefore, both the entire and fine spectra show that the heterodyne signal is broadband white chaos. Here, we adopt the bandwidth definition as the width of a frequency band, in which the power differences between the components and the spectrum peak is smaller than 3 dB. This definition can measure the bandwidth with a fixed spectral flatness of 3 dB and can also include the more prominent components. According to this definition, the bandwidths of chaotic ECL_1 and ECL_2 are only about 4.3 and 5.1 GHz. The heterodyne signal has a 3-dB bandwidth of 14.3 GHz which exceeds that of some reported amplified spontaneous emission lights [29]–[31]. As a remark, we note that an optoelectronic oscillator based on a quadrature phase-shift-keying modulator with dual feedback can generate a broad spectrum extending up to 14 GHz but has a larger spectral fluctuation of 10 dB [32]. Another oscillator based on a phase modulator has the potential for generating a featureless spectrum extending over 10 GHz but requires more sophisticated schemes to eliminate the time delay signature [33].

Having confirmed the efficacy of the approach for the generation of white chaos, attention is now turned to examining the temporal properties of the chaos. Fig. 3(a) shows the time series and the corresponding probability distribution function of the heterodyne signal and the intensity chaos of both ECLs, which were recorded by using a real-time oscilloscope with an analogue bandwidth of 6 GHz. It is quite apparent from Fig. 3(a) that the amplitude distribution of the heterodyne signal is more symmetrical than those of the ECLs. In quantitative terms the heterodyne signal has a skewness of only 0.054 which is significantly less than the skewness of the intensity chaos of ECL_1 and ECL_2, which are 0.533 and 0.267, respectively. Such a symmetric distribution is highly beneficial to achieving nearly equal numbers of ones and zeros in random number generation [2], [3].

Fig. 3(b) shows the autocorrelation functions (ACFs) of the heterodyne signal and the laser chaos, which are calculated as the expected value of $f(t) \cdot f(t - \tau_{\rm lag})$, where $f(t)$ is a time series which is offset from the mean value and then normalized by the standard deviation, and $f(t - \tau_{\rm lag})$ is a copy with a lag of $\tau_{\rm lag}$. Shown as the black and light gray lines, the correlation traces of the laser chaos exhibit obvious relaxation oscillation after the main peak at zero lag. This relaxation-oscillation signature is due to the fact that the laser relaxation oscillation dominates the intensity chaos. Additionally, each correlation trace has a distinct peak at the feedback delay, i.e., $\mathrm{ACF}_1(\tau_1) = 0.155$ and $\mathrm{ACF}_2(\tau_2) = 0.416$. That is, the ACF exposes the time-delay signature of intensity chaos of ECLs, which is actually the result of periodic modulation of the RF spectrum shown in Fig. 2(b). By contrast, the autocorrelation trace of the heterodyne signal shown as the gray (red) line no longer has peaks at the two delays: the correlation values at τ_1 and τ_2 are -2.5×10^{-4} and 1.2×10^{-4}, which are less than the standard deviation of 1.14×10^{-3} of the background noise. Furthermore, the autocorrelation trace does not have obvious relaxation oscillation like that of laser intensity chaos. These autocorrelation properties of the heterodyne signal mean that there are no signatures of time delay of ECLs and no dominant component in the heterodyne signal.

We further calculate a higher-order ACF, viz. the triple autocorrelation defined as the expected value of $f(t) \cdot f(t - \tau_{\rm lag}) \cdot f(t - \tau'_{\rm lag})$. Note that the triple autocorrelation is a two-dimensional function and for the sake of brevity we show in Fig. 3(c) cross sections of the traces obtained with $\tau'_{\rm lag} = 2\ \tau_{\rm lag}$. As plotted as the black and light gray lines, the triple correlation trace of the laser intensity chaos still has the features of the relaxation oscillation and the time delays. In contrast, shown as the gray (red) line the triple correlation of the heterodyne signal does not contain these features. The tripe correlation is approximately zero except for a small peak at zero lag whose value is the skewness of the amplitude distribution. This indicates the heterodyne signal has a flat higher-order spectrum. We mention that both the ACF and the triple correlation function of the heterodyne signal are similar to those of a white noise.

B. Effects of Feedback Strength and Frequency Detuning of Lasers

Here consideration is given to the effects of the feedback strength of ECLs and the frequency detuning of the two lasers on the spectrum and bandwidth of the heterodyne signal.

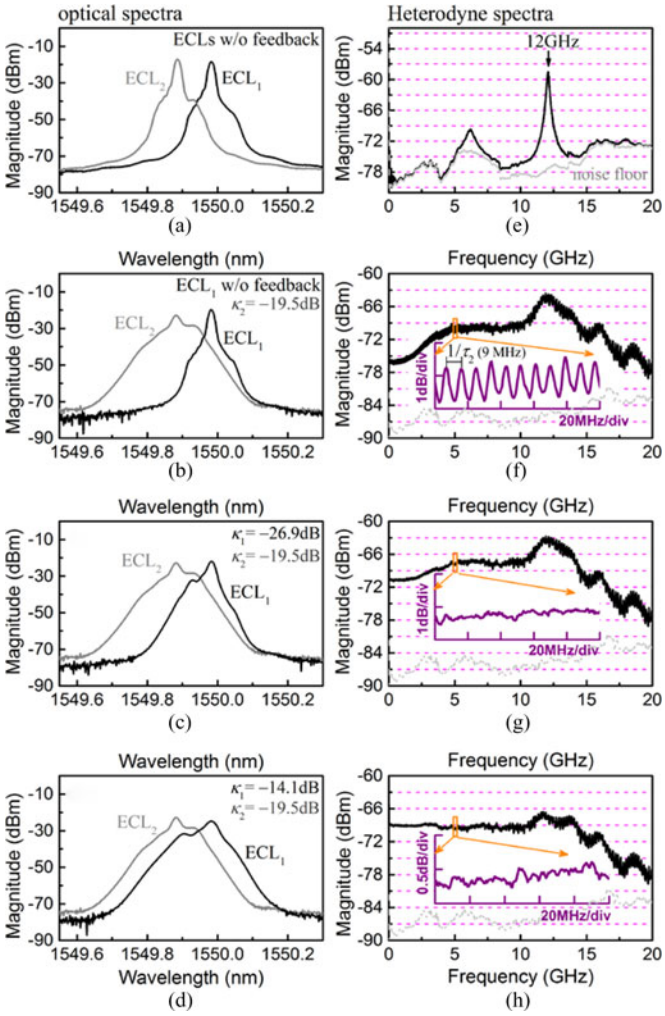

Fig. 4. (a)–(d) Experimental optical spectra of ECL_1 (black) and ECL_2 (gray) and (e)–(h) RF spectrum of the corresponding heterodyne signal: (a), (e) ECLs are both without feedback, (b), (f) ECL_1 without feedback, $\kappa_2 = -19.5$ dB, (c), (g) $\kappa_1 = -26.9$ dB, $\kappa_2 = -19.5$ dB, and (d), (h) $\kappa_1 = -14.1$ dB, $\kappa_2 = -19.5$ dB. The detuning of laser center frequencies is 12.5 GHz.

In our experiments, we examined the effects of feedback strength on the heterodyne spectrum with a fixed frequency detuning of 12.5 GHz. Some typical results are shown in Fig. 4, in which the left column includes the optical spectra of the lasers, black for ECL_1 and gray for ECL_2, and the right column presents the corresponding RF spectra of the heterodyne signals. Fig. 4(a) and (e) are the results of heterodyning of the two lasers without optical feedback. In this case, the heterodyne signal is a periodic oscillation with a center frequency near to the value of the frequency detuning, and with a linewidth of about 0.2 GHz originating from the optical phase noise of the lasers. Fig. 4(b) and (f) shows the heterodyning between ECL_1 without feedback and ECL_2 with feedback strength $\kappa_2 = -19.5$ dB. The heterodyne spectrum looks like the mirror image of the optical spectrum of ECL_2. The spectrum has an obvious peak at the beat frequency of about 12 GHz and very weak low-frequency components. In addition, as depicted in the inset, the heterodyne spectrum still has the periodic pattern or time-delay signature

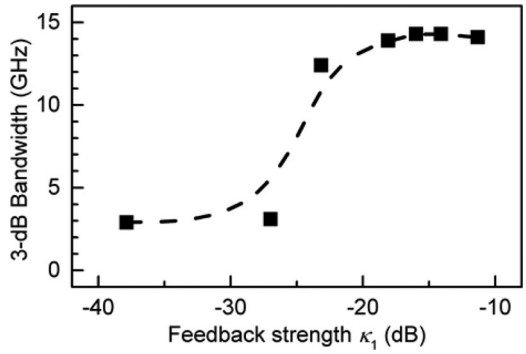

Fig. 5. Experimental bandwidth of the heterodyne signal as a function of feedback strength κ_1, obtained with $\kappa_2 = -19.5$ dB and $\nu_{c2} - \nu_{c1} = 12.5$ GHz.

of ECL_2. These results are similar to the report in [34]. It is remarked that the slight difference between the spectral peak and the laser detuning is caused by the measurement uncertainty of the optical spectrum analyzer used.

We further switched on the feedback of ECL_1 and increased its feedback strength whilst fixing κ_2 as -19.5 dB. Fig. 4(c) and (g) displays the heterodyning results obtained with $\kappa_1 = -26.9$ dB. The heterodyne spectrum is rippled and has a high peak at the beat frequency of about 12 GHz. The 3-dB bandwidth is only about 3.1 GHz. For a stronger feedback, for instance $\kappa_1 = -14.1$ dB as shown in Fig. 4(d) and (h), the heterodyne spectrum becomes flat and has a 3-dB bandwidth of about 14.6 GHz. It is worth mentioning that the heterodyne spectra in these two cases no longer have periodic modulation pattern, as shown in the insets.

By comparing the optical spectrum of ECL_1 in Fig. 4(d) with that in Fig. 4(c), one can find that strong feedback leads to a broader optical spectrum with a power-reduced center frequency. Therefore, the increase of bandwidth and the spectrum flattening due to the strong feedback can be qualitatively understood as follows. The widened optical spectrum of ECL_1 leads to more overlap with the optical spectrum of ECL_2, and then enhances low-frequency components in the optical heterodyne signal. Meanwhile, the reduced power of the center frequency of ECL_1 depresses the peak in the heterodyne spectrum, which originates from the beat between center frequencies of the lasers.

Fig. 5 shows the bandwidth of the heterodyne signal as a function of the feedback strength of ECL_1. From this figure it is seen that the bandwidth increases with gradually reduced rate for increasing optical feedback strength. As the feedback strength increases over about -23 dB, the 3-dB bandwidth can exceed 12 GHz. In addition, we mention that the external-cavity resonance or time-delay signature is always cancelled during the change of the feedback strength of ECL_1, as long as the ECMs are excited.

We further experimentally studied the effects of detuning of the lasers' frequencies on the heterodyne spectrum by changing the center wavelength or frequency of ECL_1 through a temperature controller. The center wavelength of ECL_2 was fixed at 1549.882 nm and the feedback levels were $\kappa_1 = -15.9$ dB and $\kappa_2 = -19.5$ dB. Fig. 6(a), (c) and (e) plots the optical spectra

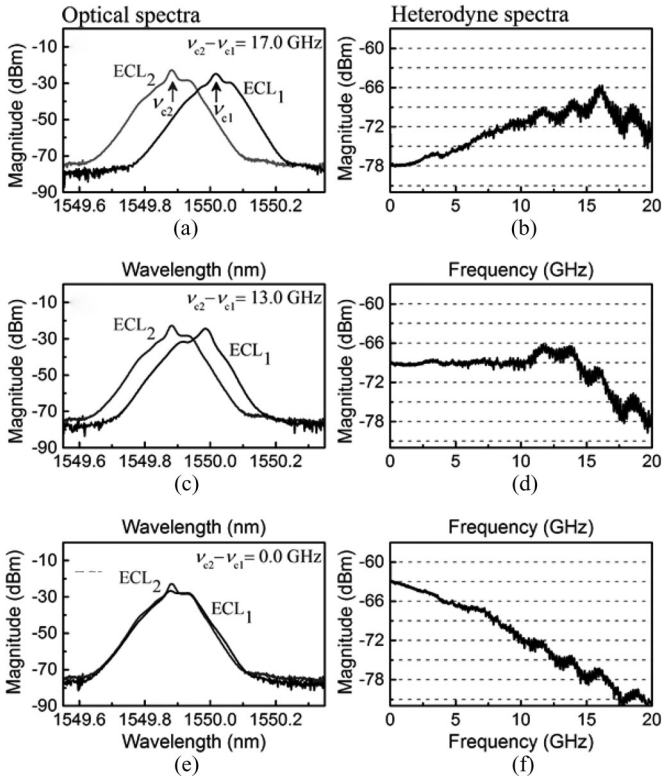

Fig. 6. (a), (c), and (e) Optical spectra of ECL_1 (black) and ECL_2 (gray) and (b), (d), and (f) RF spectra of the heterodyne signals experimentally obtained at different detuning of lasers frequencies: (a) and (b) 17.0 GHz, (c) and (d) 13.0 GHz, and (e) and (f) 0 GHz. The feedback strength $\kappa_1 = -15.9$ dB, $\kappa_2 = -19.5$ dB.

of ECL_1 and ECL_2 in black and gray lines at laser detuning of 17.0, 13.0 and 0.0 GHz, respectively; Fig. 6(b), (d) and (f) shows the corresponding RF spectra of the heterodyne signals. For the detuning of 17.0 GHz, the optical spectra of the two lasers are mainly separated, leading to an upwardly inclined profile of the heterodyne spectrum shown in Fig. 6(b). The heterodyne spectrum is contained with a power range of 12 dB and has a strong peak at the beat frequency of about 16 GHz. Its 3-dB bandwidth is only about 3.2 GHz. As the detuning is decreased to 13.0 GHz, the heterodyne signal has a flat spectrum shown in Fig. 6(d). Compared to Fig. 6(b), the spectral components with frequencies up to 10 GHz are enhanced and almost have the same power of –69 dBm. The 3-dB bandwidth is increased up to about 14 GHz. Further reducing the detuning will increase the overlap between the optical spectra, and then continue to enhance the low-frequency components of the heterodyne signal. The extreme case is zero detuning that means the two optical spectra totally overlap as shown in Fig. 6(e). Depicted in Fig. 6(f), the resultant heterodyne spectrum has a downwardly inclined profile with a small 3-dB bandwidth of 4.3 GHz, which is similar to the spectrum of the delayed self-interference signal of a chaotic ECL [27].

Fig. 7 plots the bandwidth of the heterodyne signal as a function of the frequency detuning of lasers. The results show that a flat heterodyne spectrum extending over 10 GHz can be achieved when the detuning is in a range from 10.1 to 13.2 GHz. Outside this range, larger detuning will yield a heterodyne spectrum like that in Fig. 6(b) and smaller detuning will cause a spectrum similar to that in Fig. 6(f), and thus the bandwidth reduces.

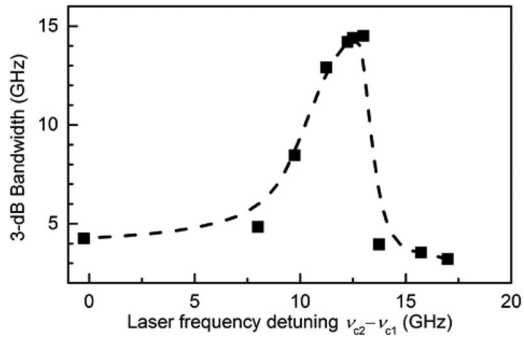

Fig. 7. Experimental bandwidth of the heterodyne signal as a function of laser frequency detuning, obtained with $\kappa_1 = -15.9$ dB and $\kappa_2 = -19.5$ dB.

IV. Theoretical Analysis

In this section we present results obtained from a theoretical model of the previously described optical heterodyne experiments. Denoting electrical field of lasers as $\boldsymbol{E}_{\rm i} = A_{\rm i}\exp[j(2\pi\nu_{0\rm i}t + \varphi_{\rm i})]$, we can express the heterodyne signal as

$$I_{\rm H} = 2A_1A_2\sin[2\pi\Delta\nu_0 t + \varphi_2(t) - \varphi_1(t)], \tag{1}$$

where $A_{\rm i}$, $\varphi_{\rm i}$, and $\nu_{0\rm i}$ ($i = 1, 2$ for ECL_1 and ECL_2) are the amplitude, phase, and solitary frequencies of the two lasers, respectively, and $\Delta\nu_0 = \nu_{02} - \nu_{01}$. The dynamical behaviors of each ECLs and hence the generation of white chaos can be explored numerically by using the following Lang–Kobayashi equations [35]

$$\begin{aligned}\dot{A}_{1,2} =\ & \frac{1}{2}(G_{1,2} - \tau_{\rm ph}^{-1})A_{1,2} + \frac{\rho_{1,2}}{\tau_{\rm in}}A_{1,2}(t-\tau_{1,2}) \\ & \times\cos\theta_{1,2} + \sqrt{\beta N_{1,2}/2\tau_{\rm N}}\xi, \end{aligned}\tag{2}$$

$$\begin{aligned}\dot{\varphi}_{1,2} =\ & \frac{\alpha}{2}(G_{1,2} - \tau_{\rm ph}^{-1}) - \frac{\rho_{1,2}}{\tau_{\rm in}}\frac{A_{1,2}(t-\tau_{1,2})}{A_{1,2}} \\ & \times\sin\theta_{1,2} + \frac{1}{A_{1,2}}\sqrt{\beta N_{1,2}/2\tau_{\rm N}}\zeta, \end{aligned}\tag{3}$$

$$\dot{N}_{1,2} = J - \tau_{\rm N}^{-1}N_{1,2} - g(N_{1,2} - N_0)A_{1,2}^2, \tag{4}$$

where, $\theta_i = 2\pi\nu_{0i}\tau_i + \varphi_i - \varphi_i(t-\tau_i)$, $G_i = g(N_i - N_0)/(1 + \varepsilon A_i^2)$, $N_{\rm i}$ is the carrier density, $\tau_{\rm i}$ is feedback delay, and $\kappa_i = 10\log_{10}(\rho_i^2)$ represents the optical feedback strength. In simulations, the intrinsic parameters of the two lasers are the same as follows. $N_0 = 0.455\times10^6\ \mu{\rm m}^{-3}$ is the transparency carrier density, $g = 1.414\times10^3\,\mu{\rm m}^3{\rm ns}^{-1}$ is the differential gain, $\varepsilon = 5\times10^{-5}\ \mu{\rm m}^3$ is the gain saturation parameter, $\tau_N = 2.5$ ns is the carrier lifetime, $\tau_{\rm ph} = 1.17$ ps is the photon lifetime, $\tau_{\rm in} = 7.38$ ps is the round-trip time in laser cavity, $\alpha = 5.0$ is the linewidth enhancement factor, $\beta = 10^{-3}$ is the spontaneous emission factor, and $J_{\rm th} = 4.239\times10^5\ \mu{\rm m}^{-3}\cdot{\rm ns}^{-1}$ is the threshold current density. The last terms in (2) and (3) denote the Gaussian noise for modeling spontaneous emission noise, where ξ and ζ are standard normal distributed random numbers.

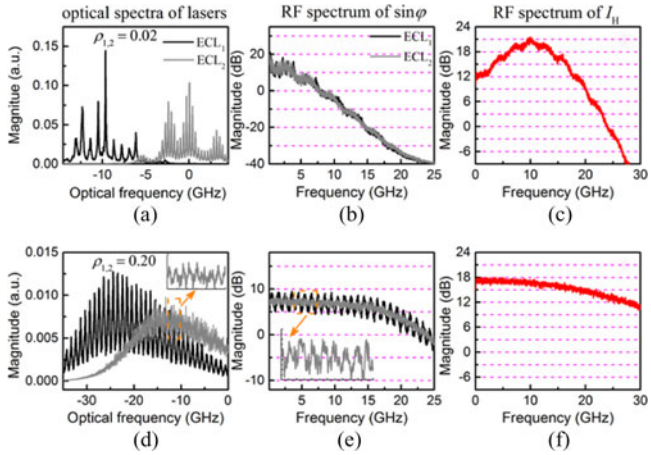

Fig. 8. Numerically simulated optical heterodyning of two ECLs: (a) optical spectra of lasers, $|\mathrm{FT}\{\mathrm{Re}(\boldsymbol{E})\}|^2$, (b) spectra of laser phase, $|\mathrm{FT}\{\sin(\varphi)\}|^2$, and (c) spectrum of the heterodyne signal, $|\mathrm{FT}\{I_{\mathrm{H}}\}|^2$, obtained with $\rho_{1,2}=0.02$; (d) optical spectra of lasers, (e) spectra of laser phase, and (f) spectrum of the heterodyne signal obtained with $\rho_{1,2}=0.20$. Here $\mathrm{FT}\{\cdot\}$ denotes Fourier transform and $\mathrm{Re}(\boldsymbol{E})$ is the real part of electrical filed. The insets in Fig. 8(d) and (e) plot the magnified spectra of ECL_2 to show the periodic pattern.

The bias current values of both lasers are set as $J=1.7J_{\mathrm{th}}$ yielding a relaxation frequency of approximately 3 GHz, the lasers' frequencies are $\nu_{01}=193.548$ THz and $\nu_{02}=193.558$ THz, and the feedback delays are $\tau_1=1.0$ ns and $\tau_2=2.77$ ns. Note the delays shorter than the experimental values are used to reduce computational overheads in storing simulation data. Also, shorter delays make it easier to observe the ECMs in optical spectrum. The rate equations are solved by fourth-order Runge–Kutta method with an integration step of 2.5 ps.

We now demonstrate two scenarios of the optical heterodyning, which are separately simulated with feedback factors $\rho_{1,2}=0.02$ and $\rho_{1,2}=0.20$, and show the corresponding results in the top and the bottom rows in Fig. 8, respectively. In Fig. 8, the first column plots the optical spectra of lasers, the second column depicts the spectra of laser phase, and the third column shows the spectra of the heterodyne signals. Note that the optical spectra are calculated as $|\mathrm{FT}\{\mathrm{Re}(\boldsymbol{E})\}|^2$, where $\mathrm{FT}\{\cdot\}$ denotes the Fourier transform and $\mathrm{Re}(\boldsymbol{E})$ is the real part of electrical field. The phase spectra are calculated as $|\mathrm{FT}\{\sin(\varphi)\}|^2$ in order to display the conversion of phase dynamics into the heterodyne signal through a sinusoidal function in (1).

Seen from the optical spectra in Fig. 8(a) and (d), the frequency detuning of the lasers is kept as 10 GHz in these two scenarios, because we set $\rho_1=\rho_2$ to ensure the two lasers have the same feedback-induced redshift in frequency or wavelength. Therefore, the optical heterodyning will yield a beat frequency of 10 GHz. In the scenario of weak feedback $\rho_{1,2}=0.02$, the heterodyne spectrum plotted in Fig. 8(c) has a high peak at the beat frequency and then is not flat. For example, in the band of 0–20 GHz, the spectrum has a large power range of about 12 dB. The 3-dB bandwidth is 8.3 GHz. This numerical heterodyne spectrum is similar to the experimental result in Fig. 4(g). The profile of this heterodyne spectrum can be understood as follows. We see from Fig. 8(a) that the two optical spectra are narrow so that they are almost separated. The narrow optical spectra mean low-frequency laser phase variation. As shown in Fig. 8(b), the phase spectra of the two lasers are flat only up to 4 GHz and then decline quickly. According to (1), the conversion of this narrow-band phase variation leads to the heterodyne spectrum shown in Fig. 8(c).

For the scenario of strong feedback $\rho_{1,2}=0.20$, the optical spectra of lasers in Fig. 8(d) are greatly broadened, which indicate more complex and fast phase dynamics. As plotted in Fig. 8(e), the spectra of laser phase extend up to 15 GHz with a slow decreasing rate and thus are much wider than the spectra in Fig. 8(b). A flat heterodyne spectrum is therefore achieved as plotted in Fig. 8(f). Its 3-dB bandwidth is about 21.6 GHz. In this spectrum, there is no longer a dominant component such as the relaxation oscillation in laser intensity chaos or like the beat frequency in Fig. 8(c). These results are in accord with the experimental results in Fig. 4(d) and (h). We also performed calculations without the noise term and obtained an almost identical heterodyne spectrum, showing that the optical phase noise of the DFB laser makes no significant contribution to the generation of the wide spectrum. Therefore, the conversion of this fast phase dynamics contributes to a wide and flat spectrum of the heterodyne signal.

Furthermore, the numerical simulations also show the elimination of the signature of external-cavity resonance or the time-delay signatures of ECLs, which is achieved in the experiments. Consider the scenario of $\rho_{1,2}=0.20$ as an example. Shown as the black curve in Fig. 8(d), the optical spectrum of ECL_1 is like a comb spectrum consisting of ECMs with a span of $1/\tau_1$, i.e., 1 GHz. The RF spectrum (not shown) of intensity chaos of ECL_1 has a feature of periodic modulation with a period of 1 GHz, similar to the experimental spectrum of ECLs plotted in Fig. 2(b). Additionally, the spectrum of laser phase shown as the black curve in Fig. 8(e) also has a modulation feature due to the coupling between laser intensity and phase. Note that the ECL_2 has similar spectral periodic feature as shown in the inset. As shown in Fig. 8(f), the heterodyne spectrum does not have any periodic modulation, which agrees with the experimental heterodyne spectrum in Fig. 2(b).

We attribute the elimination of the signature of external-cavity resonance to the non-resonant beatings between two sets of ECMs with different frequency spans. We firstly analyze the reason of the signature appearing in spectrum of laser intensity chaos. Laser intensity is measured by square-low detection of optical field and thus consists of beats among ECMs. For instance, the intensity of ECL_1 includes the beats between ECMs $\nu_p=p/\tau_1$ and $\nu_{p'}=p'/\tau_1$. All the beats are resonant at frequencies of $f_{\mathrm{m}}=m/\tau_1$, where $m=1,2,3,\ldots$, and then leads to the periodically modulated spectrum. For the heterodyne signal, there is only the beating between the two laser fields. Considering the ECMs of ECL_1 and ECL_2 as $\nu_p=p/\tau_1$ and $\nu_q=q/\tau_2$, respectively, we can deduce the beat frequencies between the two sets of ECMs as $f_{pq}=p/\tau_1-q/\tau_2$. For arbitrary integer pairs (p, q) and (p', q'), one can get $f_{pq}\neq f_{p'q'}$ under the condition of that the two delays are incommensurate, which leads to $(q-q')\tau_1\neq(p-p')\tau_2$. This means that all of the beat frequencies between the two sets of ECMs are different, which we call non-resonant beatings. Because of these non-resonant beats,

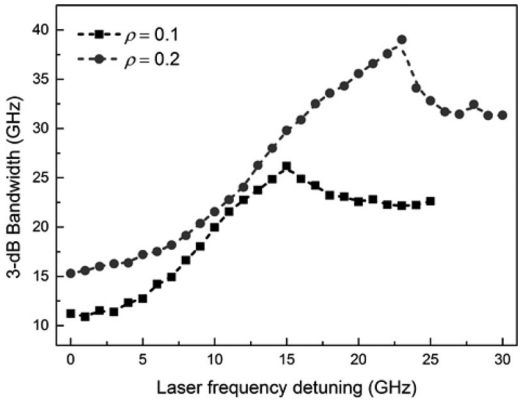

Fig. 9. Numerically obtained bandwidth of the heterodyne signal as a function of detuning of lasers' frequencies, obtained with $\rho_{1,2} = 0.10$ (squares) and $\rho_{1,2} = 0.20$ (circles), respectively.

the heterodyne spectrum no longer has the pattern of periodic modulation that appears in laser intensity chaos.

We mention that the concealment of the feature of external-cavity resonance or time-delay signature can also be understood from the viewpoint of autocorrelation. Because the two chaotic lasers are independent, the ACF of the heterodyne signal I_{H} is not larger than the product of the ACFs of laser amplitudes $A_{1,2}$. Under the condition $q\tau_1 \neq p\tau_2$, $\mathrm{ACF}_1(p\tau_2)$ and $\mathrm{ACF}_2(q\tau_1)$ are approximately equal to zero, and thus their product conceals the correlation at the delay values. Actually, the condition can be relaxed. Because the number of correlation peaks of laser chaos is finite, $q\tau_1 = p\tau_2$ with large enough integers p and q can also eliminate the correlation peaks, i.e., signatures of feedback delays, for instance $p/q = 100/277$ in the simulations and 853/1107 in the experiments.

In addition, we have numerically analyzed the effects of laser detuning on the bandwidth of the heterodyne signal. It is mentioned that we used a data length of 2×10^6 points to calculate the RF spectrum and then employed a FFT (fast Fourier transform) smoothing method to separate random fluctuation from the spectrum. Then we calculated the bandwidth from the smoothed spectrum.

Fig. 9 plots the 3-dB bandwidth of the heterodyne signal as function of laser frequency detuning. Squares and circles present the results obtained with $\rho_{1,2} = 0.10$ and $\rho_{1,2} = 0.20$, respectively. The same tendency can be found: as detuning increases, the bandwidth experiences a slow increase, and then a rapid growth followed by a sudden decreasing. The numerical heterodyne spectrum exhibits a similar evolution that changes from Fig. 6(f) to (d) and then to (b). During this evolution, a spectral peak at the beat frequency appears and grows. When the peak exceeds the lowest-frequency component more than 3 dB, the bandwidth stops increasing and drops. This tendency agrees with the experimental results shown in Fig. 7. Note that, for large detuning, the bandwidth decrease in experiments is greater than that in the simulation. The reason is that the experimental optical spectra of lasers are narrower so that the peak in heterodyne spectrum has a smaller bandwidth. In addition, comparison between the two simulated results in Fig. 9 shows again that a higher bandwidth can be achieved by increasing feedback strength because strong feedback leads to a fast and wideband laser phase dynamics.

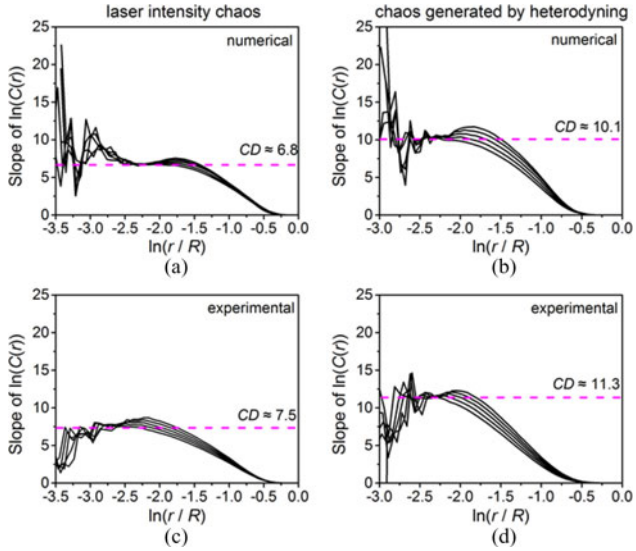

Fig. 10. CD analysis for (a) and (c) the laser intensity chaos and (b) and (d) the heterodyne signal by the slope of the logarithmic plot of the correlation integral $C(r)$. Plots (a) and (b) are results for the numerical intensity chaos of ECL_1 in Fig. 8(d) and the heterodyne signal in Fig. 8(f); plots (c) and (d) are results for the experimental intensity chaos of ECL_1 and the heterodyne signal in Fig. 2. The horizontal coordinates are normalized by the diameter R of the reconstructed attractor.

V. Discussion

In order to explore further the approach taken, we utilize correlation dimensional analysis to show that the generated white chaos is high-dimensional by using the Grassberger–Procaccia (GP) algorithm [36]. The algorithm counts the correlation integral $C(r)$ that is the probability of pairs of points with a Euclidean distance not larger than r in a delay-embedded phase space and estimates the CD by the converged slope of logarithmic plots of $C(r)$ versus r. Note that, for a data length of M points the estimation bound of CD is given by $2\ln(M)/\ln(R/r)$ [37], where R is the diameter of the reconstructed attractor. For comparison we have analyzed the intensity chaos and the white chaos obtained by the optical heterodyning both in simulations and experiments. For the numerical intensity chaos of ECL_1 in the state plotted in Fig. 8(d), the GP results obtained with a data length $M = 30\,000$ points are given in Fig. 10(a). A clear scaling region of $\ln(r/R)$ is recognized between -2.5 and -2.1, yielding a dimension CD ≈ 6.8. Considering that the white chaos has a flat and wide power spectrum and may thus have higher dimensionality, we increase the data length to 50 000 points to attempt estimation for the white chaos. Fig. 10(b) depicts the results for the heterodyne signal shown in Fig. 8(f), and shows that a plateau still appears but in a smaller scaling region from -2.3 and -2.1. The plateau indicates the dimension of the numerical white chaos as approximately 10.1, which is very close to the estimation bound of 10.3. Note that the calculated dimension of the numerical laser phase $\sin\varphi$ is about 7.2, meaning the laser phase is chaotic. Therefore, the reason for the high dimension of the heterodyne signal appears to be that the product of chaotic

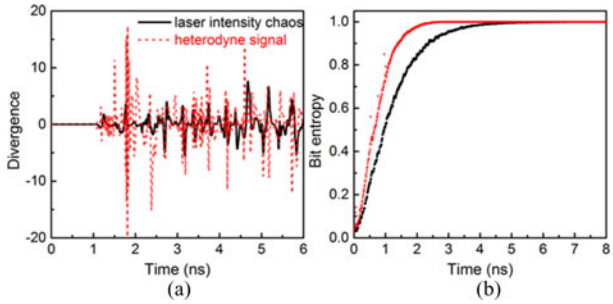

Fig. 11. (a) Divergence of two temporal waveforms numerically generated at the same initial conditions when different noise sequences are added at $t = 0$; (b) Bit entropy as a function of time. Gray (red online), the heterodyne signal; black, laser chaos.

motions, the intensity chaos and the phase chaos, yields a more complex attractor.

For experimental chaos, to reduce the influence of detection noise, we have employed a re-embedding method that applies the GP algorithm on the principal components obtained by singular value decomposition on time series [38]. The results of the experimental intensity chaos of ECL_1 and the heterodyne signal shown in Fig. 2 are plotted in Fig. 10(c) and (d), respectively. Similar to the numerical results, the white chaos generated by optical heterodyning has a higher dimensionality than the laser intensity chaos. We mention that for the experimental white chaos the CD of 11.3 actually exceeds the estimation bound, implying a higher dimensionality. Accurate estimation of the dimension for the experimental white chaos requires a huge dataset and a time-consuming re-embedding method, and thus is difficult. It is therefore believed that the high-dimensional white chaos can be robust against possible phase-space reconstruction.

We also numerically compare the sensitivity to initial conditions between the heterodyne chaos and the ECL_1 chaos under the conditions of Fig. 8(d) and (f). As shown in Fig. 11(a), due to intrinsic noise, both of their trajectories starting at the same initial conditions diverge after about 1.2 ns. Different noise cases give different chaotic time series. Fig. 11(b) plots the average time-dependent entropy calculated from 10^6 time series (10^3 different noise instances for each initial condition $\times 10^3$ different initial conditions) [5]. One can see that the bit entropy for the heterodyne chaos increases more quickly. Note that the memory time of initial conditions is defined as the time for the entropy to reach 0.995 which is a value corresponding to the pass criteria of the 0/1 ratio test in the NIST tests of randomness [39]. The heterodyne chaos has a memory time of about 2.44 ns shorter than the value of 5.08 ns for the laser chaos. This means the heterodyne chaos is faster than laser chaos in terms of sensitivity to initial conditions. This, we conjecture, is due to that the heterodyne chaos mainly originating from phase-to-intensity conversion being more sensitive to phase noise.

Using this heterodyne chaos to generate random numbers is reserved for further work and is outside the scope of this paper. Here, we would like to discuss the benefits of using the optical heterodyne signal. For single-bit extraction, considering the result in [40] that a laser chaos with a flat spectrum covering a frequency range from 6–16 GHz generates 8.33 Gb/s random bits, the proposed heterodyne signal with 14 GHz bandwidth could provide a single-bit generation rate greater than 10 Gb/s. For multi-bit extraction, as indicated by our previous work about the delayed self-interference signal [27], the symmetric amplitude distribution and free of time-delay signature can increase the number of least significant bits passing the NIST tests without XOR processing and then further improve the generation rate.

It is also worth mentioning that the heterodyne chaos can also improve the performance of radar [41], [42]. Its broadband white spectrum can enhance the spatial resolution and anti-jamming ability of radar detection.

Finally, we discuss the influence of the mismatch between the lengths of the two fiber paths between the 3 dB fiber coupler and the balanced detector in the setup. In principle, the two fiber paths should have the same length so that the laser intensity chaos can be subtracted totally. Otherwise, the residue of laser chaos leads to the appearance of time-delay signatures. We have simulated the effects of optical path difference on the time-delay signatures, and have found that a suitable optical path difference should ensure the correlation of laser chaos and its delayed duplicate higher than 0.95. For the scenario of $\rho_{1,2} = 0.20$ in Fig. 8, an optical path difference smaller than 1.5 mm is required.

VI. Conclusion

To sum up, we experimentally and numerically demonstrate that the optical heterodyning of two ECLs can generate physical white chaos. Chaos with a colorless spectral bandwidth of 14 GHz is experimentally achieved. The generated chaos does not have the signatures of laser relaxation oscillation and external-cavity resonance which exist in the dynamics of the ECLs. The time series of the white chaos has a high CD greater than 10, a symmetric amplitude distribution, and a delta-like ACF similar to that of white noise. All of these statistical characteristics are of beneficial to random number generation as well as radar detection. In addition, our results are expected to be of research interest in the generation of white noise using physical chaos [26], [43].

Acknowledgment

A. B. Wang would like to thanks Prof. I. Fischer, for his helpful comments and suggestions.

References

[1] A. Uchida *et al.*, "Fast physical random bit generation with chaotic semiconductor lasers," *Nature Photon.*, vol. 2, no. 227, pp. 728–732, 2008.
[2] I. Reidler, Y. Aviad, M. Rosenbluh, and I. Kanter, "Ultrahigh-speed random number generation based on a chaotic semiconductor laser," *Phys. Rev. Lett.*, vol. 103, no. 2, pp. 024102-1–024102-4, 2009.
[3] I. Kanter, Y. Aviad, I. Reidler, E. Cohen, and M. Rosenbluh, "An optical ultrafast random bit generator," *Nature Photon.*, vol. 4, no. 1, pp. 58–61, 2010.
[4] M. Virte, E. Mercier, H. Thienpont, K. Panajotov, and M. Sciamanna, "Physical random bit generation from chaotic solitary laser diode," *Opt. Exp.*, vol. 22, no. 14, pp. 17271–17280, 2014.
[5] T. Mikami *et al.*, "Estimation of entropy rate in a fast physical random-bit generator using a chaotic semiconductor laser with intrinsic noise," *Phys. Rev. E*, vol. 85, no. 1, pp. 016211-1–016211-7, 2012.

[6] R. Sakuraba, K. Iwakawa, K. Kanno, and A. Uchida, "Tb/s physical random bit generation with bandwidth-enhanced chaos in three-cascaded semiconductor lasers," *Opt. Exp.*, vol. 23, no. 2, pp. 1470–1490, 2015.
[7] A. B. Wang, Y. C. Wang, and H. He, "Enhancing the bandwidth of the optical chaotic signal generated by a semiconductor laser with optical feedback," *IEEE Photon. Technol. Lett.*, vol. 20, no. 19, pp. 1633–1635, Oct. 2008.
[8] K. Hirano *et al.*, "Characteristics of fast physical random bit generation using chaotic semiconductor lasers," *IEEE J. Quantum Electron.*, vol. 45, no. 11, pp. 1367–1379, Nov. 2009.
[9] D. Rontani, A. Locquet, M. Sciamanna, D. S. Citrin, and S. Ortin, "Time-delay identification in a chaotic semiconductor laser with optical feedback: a dynamical point of view," *IEEE J. Quantum Electron.*, vol. 45, no. 7, pp. 879–891, Jul. 2009.
[10] Y. Wu, Y. C. Wang, P. Li, A. B. Wang, and M. J. Zhang, "Can fixed time delay signature be concealed in chaotic semiconductor laser with optical feedback?" *IEEE J. Quantum Electron.*, vol. 48, no. 11, pp. 1371–1379, Nov. 2012.
[11] K. Hirano *et al.*, "Fast random bit generation with bandwidth-enhanced chaos in semiconductor lasers," *Opt. Exp.*, vol. 18, no. 6, pp. 5512–5524, 2010.
[12] Y. Akizawa *et al.*, "Fast random number generation with bandwidth-enhanced chaotic semiconductor lasers at 8×50 Gb/s," *IEEE Photon. Technol. Lett.*, vol. 24, no. 12, pp. 1042–1044, Jun. 2012.
[13] X. Z. Li and S. C. Chan, "Random bit generation using an optically injected semiconductor laser in chaos with oversampling," *Opt. Lett.*, vol. 37, no. 11, pp. 2163–2165, 2012.
[14] A. B. Wang, Y. C. Wang, and J. F. Wang, "Route to broadband chaos in a chaotic laser diode subject to optical injection," *Opt. Lett.*, vol. 34, no. 8, pp. 1144–1146, 2009.
[15] Y. Takiguchi, K. Ohyagi, and J. Ohtsubo, "Bandwidth-enhanced chaos synchronization in strongly injection-locked semiconductor lasers with optical feedback," *Opt. Lett.*, vol. 28, no. 5, pp. 319–321, 2003.
[16] A. Uchida, T. Heil, Y. Liu, P. Davis, and T. Aida, "High-frequency broadband signal generation using a semiconductor laser with a chaotic optical injection," *IEEE J. Quantum Electron.*, vol. 39, no. 11, pp. 1462–1467, Nov. 2003.
[17] M. J. Zhang *et al.*, "Generation of broadband chaotic laser using dual-wavelength optically injected Fabry–Pérot laser diode with optical feedback," *IEEE Photon. Technol. Lett.*, vol. 23, no. 24, pp. 1872–1874, Dec. 2011.
[18] Y. Hong, P. S. Spencer, and K. A. Shore, "Enhancement of chaotic signal bandwidth in vertical-cavity surface-emitting lasers with optical injection," *J. Opt. Soc. Amer. B*, vol. 29, no. 3, pp. 415–419, 2012.
[19] A. B. Wang *et al.*, "Generation of flat-spectrum wideband chaos by fiber ring resonator," *Appl. Phys. Lett.*, vol. 102, no. 3, pp. 031112-1–031112-5, 2013.
[20] D. Rontani, A. Locquet, M. Sciamanna, and D. S. Citrin, "Loss of time-delay signature in the chaotic output of a semiconductor laser with optical feedback," *Opt. Lett.*, vol. 32, no. 20, pp. 2960–2962, 2007.
[21] J. G. Wu, G. Q. Xia, and Z. M. Wu, "Suppression of time delay signatures of chaotic output in a semiconductor laser with double optical feedback," *Opt. Exp.*, vol. 17, no. 22, pp. 20124–20133, 2009.
[22] N. Oliver, M. C. Soriano, D. W. Sukow, and I. Fischer, "Dynamics of a semiconductor laser with polarization-rotated feedback and its utilization for random bit generation," *Opt. Lett.*, vol. 36, no. 23, pp. 4632–4634, 2011.
[23] H. Lin, Y. Hong, and K. A. Shore, "Experimental study of time-delay signatures in vertical-cavity surface-emitting lasers subject to double-cavity polarization-rotated optical feedback," *J. Lightw. Technol.*, vol. 32, no. 9, pp. 1829–1836, May 2014.
[24] S. S. Li, Q. Liu, and S. C. Chan, "Distributed feedbacks for time-delay signature suppression of chaos generated from a semiconductor laser," *IEEE J. Photon.*, vol. 4, no. 5, pp. 1930–1935, Oct. 2012.
[25] T. Kohda and S. Kajihara, "Design of piecewise-linear Markov maps generating white chaos: An inverse problem of dynamical systems," in *Proc. IEEE Int. Symp. Circuits Syst.*, 1992, vol. 6, pp. 2805–2808.
[26] G. C. McGonigal and M. I. Elmasry, "Generation of noise by electronic iteration of the logistic map," *IEEE Trans. Circuits Syst.*, vol. 34, no. 8, pp. 981–983, Aug. 1987.
[27] A. B. Wang *et al.*, "Generation of wideband chaos with suppressed time-delay signature by delayed self-interference," *Opt. Exp.*, vol. 21, no. 7, pp. 8701– 8710, 2013.
[28] L. Goldberg, H. F. Taylor, A. Dandridge, J. F. Weller, and R. Miles, "Spectral characteristics of semiconductor lasers with optical feedback," *IEEE Trans. Microw. Theory Tech.*, vol. 30, no. 4, pp. 401–410, Apr. 1982.
[29] C. R. Williams, J. C. Salevan, X. Li, R. Roy, and T. E. Murphy, "Fast physical random number generator using amplified spontaneous emission," *Opt. Exp.*, vol. 18, no. 23, pp. 23584–23597, 2010.
[30] X. Li, A. B. Cohen, T. E. Murphy, and R. Roy, "Scalable parallel physical random number generator based on a superluminescent LED," *Opt. Lett.*, vol. 36, no. 6, pp. 1020–1022, 2011.
[31] A. Argyris, E. Pikasis, S. Deligiannidis, and D. Syvridis, "Sub-Tb/s physical random bit generators based on direct detection of amplified spontaneous emission signals," *J. Lightw. Technol.*, vol. 30, no. 9, pp. 1329–1334, May 2012.
[32] M. Nourine, Y. K. Chembo, and L. Larger, "Wideband chaos generation using a delayed oscillator and a two-dimensional nonlinearity induced by a quadrature phase-shift-keying electro-optic modulator," *Opt. Lett.*, vol. 36, no. 15, pp. 2833–2835, 2011.
[33] R. M. Nguimdo, P. Colet, L. Larger, and L. Pesquera, "Digital key for chaos communication performing time delay concealment," *Phys. Rev. Lett.*, vol. 107, no. 3, pp. 034103-1–034103-4, 2011.
[34] D. Brunner, X. Porte, M. C. Soriano, and I. Fischer, "Real-time frequency dynamics and high-resolution spectra of a semiconductor laser with delayed feedback," *Sci. Rep.*, vol. 2, pp. 732-1–732-5, 2012.
[35] R. Lang and K. Kobayashi, "External optical feedback effects on semiconductor injection laser properties," *IEEE J. Quantum Electron.*, vol. 16, no. 3, pp. 347–355, Mar. 1980.
[36] P. Grassberger and I. Procaccia, "Characterization of strange attractors," *Phys. Rev. Lett.*, vol. 50, no. 5, pp. 346–349, 1983.
[37] J. P. Eckmann and D. Ruelle, "Fundamental limitations for estimating dimensions and Lyapunov exponents in dynamical systems," *Phys. D*, vol. 56, no. 2, pp. 185–187, 1992.
[38] K. Fraedrich and R. Wang, "Estimating the correlation dimension of an attractor from noisy and small datasets based on re-embedding," *Phys. D*, vol. 65, no. 4, pp. 373–398, 1993.
[39] A. Rukhin *et al.*, "A statistical test suite for random and pseudorandom number generators for cryptographic applications," National Institute of Standards and Technology, (NIST)Gaithersburg, MD, USA, Tech. Rep. SP 800-22 Rev. 1a, 2010.
[40] T. Yamazaki and A. Uchida, "Performance of random number generators using noise-based superluminescent diode and chaos-based semiconductor lasers," *IEEE J. Sel. Topics Quantum Electron.*, vol. 19, no. 4, pp. 0600309-1–0600309-9, Jul./Aug. 2013.
[41] F. Y. Lin and J. M. Liu, "Chaotic radar using nonlinear laser dynamics," *IEEE J. Quantum Electron.*, vol. 40, no. 6, pp. 815–820, Jun. 2004
[42] F. Y. Lin and J. M. Liu, "Chaotic lidar," *IEEE J. Sel. Topics Quantum Electron.*, vol. 10, no. 5, pp. 991–997, Sep./Oct. 2004.
[43] R. L. Kautz, "Using chaos to generate white noise," *J. Appl. Phys.*, vol. 86, no. 10, pp. 5794–5800, 1999.

Anbang Wang (M'14) received the B.S. degree in applied physics and the Ph.D. degree in electronic circuits and systems from the Taiyuan University of Technology, Taiyuan, China, in 2003 and 2014, respectively.

In 2006, he joined the Taiyuan University of Technology, where he is currently an Assistant Professor with the College of Physics and Optoelectronics. He is also a Visiting Scholar with the School of Electronic Engineering, Bangor University, Bangor, U.K. His research interests include laser dynamics, wideband chaos generation, optical time-domain reflectometry, and random bit generation.

Bingjie Wang received the Ph.D. degree in electronic circuits and systems from the Taiyuan University of Technology, Taiyuan, China, in 2012.

She is currently an Associate Professor with the College of Physics and Optoelectronics, Taiyuan University of Technology. Her current research interests include laser dynamics and wire health monitoring using chaotic signal.

Lei Li received the B.S. degree in optical information sciences and technology and the M.S. degree in optical engineering from the Taiyuan University of Technology, Taiyuan, China, in 2011 and 2014, respectively.

His research interest includes the random number generation using wideband chaos.

Yuncai Wang received the B.S. degree in semiconductor physics from Nankai University, Tianjin, China, in 1986, and the M.S. degree in physics and the Ph.D. degree in optics from the Xi'an Institute of Optics and Precision Mechanics, Chinese Academy of Sciences, Xi'an, China, in 1994 and 1997, respectively.

He joined the Taiyuan University of Technology (TUT), Taiyuan, China, in 1986, where he became an Assistant Professor in 1994, Associate Professor in 1998, and Professor in 2003. From 2001 to 2002, he was a Visiting Researcher with the Institute of Solid State Physics, Technical University of Berlin, Berlin, Germany. He has served as the Head of the College of Physics and Optoelectronics, TUT. He is currently the Director at the Key Laboratory of Advanced Transducers and Intelligent Control System, Ministry of Education, Taiyuan University of Technology. He has authored/coauthored more than 100 journal/conference publications and ten patents. His recent research interests include secure communications, random number/code generation, fiber sensing, and application of laser dynamics.

Dr. Wang is a Fellow of the Chinese Instrument and Control Society, and a Senior Member at the Chinese Optical Society and the Chinese Physical Society. He is a Program Member at the International Workshop on Chaos-Fractals Theories and Applications, and was a Coorganizer at the sixth workshop held in Taiyuan, China, in August 2013. He organized a special session for the 35th conference of the Progress in Electromagnetics Research Symposium held in Guangzhou, China, in August 2014.

K. Alan Shore (M'88–SM'95) received the B.A. degree in mathematics from the University of Oxford, Oxford, U.K., and the Ph.D. degree in applied mathematics from University College, Cardiff, U.K.

He was a Lecturer with the University of Liverpool, Liverpool, U.K., from 1979 to 1983. He joined the University of Bath, Bath, U.K., where he became a Senior Lecturer in 1986, Reader in 1990, and Professor in 1995. He was a Visiting Researcher with the Center for High Technology Materials, University of New Mexico, Albuquerque, NM, USA, in 1987, and the Huygens Laboratory, Leiden University, Leiden, The Netherlands, in 1989. From 1990 to 1991, he was with the Teledanmark Research Laboratory and the Modeling, Nonlinear Dynamics and Irreversible Thermodynamics Center, Technical University of Denmark, Lyngby, Denmark. He was a Guest Researcher with the Electrotechnical Laboratory Tsukuba, Japan, in 1991. He was a Visiting Professor with the Department of Physics, University de les Illes Balears, Palma de Mallorca, Spain, in 1992. He was appointed as the Chair of Electronic Engineering, University of Wales, Bangor, U.K., in 1995, where he has served as the Head of the School of Informatics and the College of Physical and Applied Sciences. He was the Director of Industrial and Commercial Optoelectronics, a Welsh Development Agency Centre of Excellence. From 1996 to 1998, he was a Visiting Lecturer with the Instituto de Fisica de Cantabria, Santander, Spain. In 1996, 1998, 2000, 2002, 2005, and 2008, he was a Visiting Researcher with the Department of Physics, Macquarie University, Sydney, Australia. In 2001, he was a Visiting Researcher with the ATR Adaptive Communications Laboratories, Kyoto, Japan. He held a JSPS Invitation Fellowship with the Nara Institute of Science and Technology, Nara, Japan, in 2011. He has been the Chair of Welsh Optoelectronics Forum and he is currently the Chair of the Photonics Academy for Wales, Bangor. He is the author or coauthor of more than 930 contributions to archival journals, books, and technical conferences. He is a Coeditor with Prof. D. Kane of the research monograph *Unlocking Dynamical Diversity* (Wiley, 2005). His current research interests include semiconductor optoelectronic device design and experimental characterization with particular emphasis on nonlinearities in laser diodes dynamics, vertical cavity semiconductor lasers, and applications of nonlinear dynamics in semiconductor lasers to optical data encryption.

Dr. Shore is a Program Member of several Optical Society of America conferences and was a Coorganizer of the Rank Prize Symposium on Nonlinear Dynamics in Lasers held in the Lake District, U.K., in August 2002. He was a Cofounder, Organizer, and till 2012, Program Committee Chair of the International Conference on Semiconductor and Integrated Optoelectronics, which, since 1987, has been held annually in Cardiff, Wales, U.K. He is a Fellow of the Optical Society of America, the Institute of Physics, and the Learned Society of Wales for which he serves as a Council Member since 2012.